Hydrophobic Barriers of Lipid Bilayer Membranes Formed by Reduction of Water Penetration by Alkyl Chain Unsaturation and Cholesterol

ARTICLE *in* BIOCHEMISTRY · JULY 1994

Impact Factor: 3.02 · DOI: 10.1021/bi00190a022 · Source: PubMed

Hydrophobic Barriers of Lipid Bilayer Membranes Formed by Reduction of Water Penetration by Alkyl Chain Unsaturation and Cholesterol†

Witold K. Subczynski,*,‡,§ Anna Wisniewska,‡,§ Jun-Jie Yin,§ James S. Hyde,§ and Akihiro Kusumi*,⊥

Biophysics Department, Institute of Molecular Biology, Jagiellonian University, Krakow, Poland, National Biomedical ESR Center, Biophysics Research Institute, Medical College of Wisconsin, Milwaukee, Wisconsin 53226, and Department of Pure and Applied Sciences, The University of Tokyo, Meguro-ku, Tokyo 153, Japan

Received February 1, 1994; Revised Manuscript Received April 15, 1994®

ABSTRACT: The hydrophobicity profiles across phosphatidylcholine (PC)–cholesterol bilayer membranes were estimated in both frozen liposome suspensions and fluid-phase membranes as a function of alkyl chain length, unsaturation, and cholesterol mole fraction. A series of stearic acid spin labels, with the probe attached to various positions along the alkyl chain, cholesterol-type spin labels (cholestane and androstane spin labels), and Tempo–PC were used to examine depth-dependent changes in local hydrophobicity, which is determined by the extent of water penetration into the membrane. Local hydrophobicity was monitored primarily by observing the *z* component of the hyperfine interaction tensor (A_z) of the nitroxide spin probe in a frozen suspension of the membrane at −150 °C and was further confirmed *in the fluid phase* by observing the rate of collision of $Fe(CN)_6^{3-}$ with the spin probe in the membrane using saturation recovery ESR. Saturated-PC membranes show low hydrophobicity (high polarity) across the membrane, comparable to 2-propanol and 1-octanol, even at the membrane center where hydrophobicity is highest. Longer alkyl chains only make the central hydrophobic regions wider without increasing the level of hydrophobicity. Introduction of a double bond at C9–C10 *decreases* the level of water penetration at all locations in the membrane, and this effect is considerably greater than the *cis* configuration than with the *trans* configuration. Incorporation of cholesterol (30 mol %) dramatically changes the profiles; it *decreases* hydrophobicity (increases water penetration) from the polar headgroup region to a depth of approximately C7 and C9 for saturated- and unsaturated-PC membranes, respectively, which is about where the bulky rigid steroid ring structure of cholesterol reaches in the membrane. Membrane hydrophobicity sharply increases at these positions from the level of methanol to the level of pure hexane, and hydrophobicity is constant in the inner region of the membrane. Thus, formation of effective hydrophobic barriers to permeation of small polar molecules requires alkyl chain unsaturation and/or cholesterol. The thickness of this rectangular hydrophobic barrier is less than 50% of the thickness of the hydrocarbon regions. Results obtained in dioleoyl-PC–cholesterol membranes in the fluid phase are similar to those obtained in frozen membranes. These results correlate well with permeability data for water and amino acids in the literature.

One of the most fundamental properties of biological membranes is that they act as a barrier to permeation of polar molecules. This barrier effect is largely due to the hydrophobicity of the membrane interior. Since the dielectric constant in the hydrocarbon phase is expected to be low (Griffith et al., 1974), a considerable amount of free energy would be required to move an ion from the aqueous phase into the hydrocarbon phase in the membrane.

Despite the importance of this hydrophobic barrier in determining the permeability of small solutes, it has been disregarded in many studies that tried to relate the membrane structure to permeability. Most of these studies focused on membrane fluidity, probably because hydrophobicity profiles across the membrane had not yet been studied in sufficient detail [for example, Milon et al. (1986), Lazrak et al. (1987), Higaki et al. (1988), Koenig et al. (1992), Bassolino-Klimas et al. (1993)]. Thus, we have undertaken a comprehensive investigation of the profiles of hydrophobic barriers of model membranes. We have obtained hydrophobic profiles of membranes consisting of various phosphatidylcholines (PCs[1])- and cholesterol as a function of alkyl chain length, unsaturation, and cholesterol mole fraction.

Hydrophobicity in the membrane is largely determined by the extent of water penetration into the membrane, since dehydration abolishes the hydrophobic gradient in liposome samples (Griffith et al., 1974). The specific meaning of "hydrophobicity" depends on the method used to evaluate hydrophobicity.

Four types of techniques have been employed to monitor spatial variations in hydrophobicity across the membrane.

(1) Neutron diffraction provides direct information on the depth of water penetration into the phospholipid bilayer with a high level of spatial resolution (4.5 Å; Zaccai et al., 1975; Franks & Lieb, 1979; Blechner et al., 1990). However, the actual level of water penetration is difficult to evaluate since a "zero level" for water distribution cannot be determined from the diffraction results (Franks & Lieb, 1980). Fur-

† This work was supported in part by U.S. Public Health Service Grants GM22923 and RR01008 and by Grants-in-Aid from the Ministry of Education, Science, and Culture of Japan.

‡ Jagiellonian University.
§ Medical College of Wisconsin.
⊥ The University of Tokyo.

® Abstract published in *Advance ACS Abstracts,* June 1, 1994.

[1] Abbreviations: A_0, isotropic hyperfine constant of the nitroxide spin probe; A_z, *z*-component of the hyperfine interaction tensor of the nitroxide spin probe; ASL, androstane spin label; CSL, cholestane spin label; DXPC (where X = L, M, P, S, O, and E), dilauroyl-, dimyristoyl-, dipalmitoyl-, distearoyl-, dioleoyl-, and dielaidoylphosphatidylcholine, respectively; EYPC, egg-yolk phosphatidylcholine; *n*-SASL, *n*-doxylstearic acid spin label (*n* = 5, 7, 9, 10, 12, or 16); PC, L-α-phosphatidylcholine; T-PC, tempocholine phosphatidic acid ester.

0006-2960/94/0433-7670$04.50/0

thermore, these neutron diffraction studies failed to show spatial variations in water concentration within the membrane hydrocarbon region, probably because diffraction data are not sufficiently sensitive to the presence of very low concentrations of water in the hydrocarbon phase, and the total water content of the sample is only 10% by weight. With this technique, measurements were carried out for membranes in the gel phase.

(2) Capacitance measurements of planar bilayers have been used to characterize the hydrophobic barrier of the membrane. However, such measurements are unable to provide detailed features of the hydrophobicity profiles because they assume that the barrier is rectangular, i.e., a relatively constant dielectric constant across the hydrocarbon region of the bilayer and sharp changes in the dielectric constant at the hypothesized "depth of water penetration" (Andrews et al., 1971; White, 1977; Simon et al., 1982; we will show that this is true only in special cases).

(3) Fluorescence methods have been used in which fluorescent probes are placed at various "depths" in the membrane and water (and heavy water)-induced spectral shifts and fluorescence lifetime decay are observed (Chaplin & Kleinfeld, 1983; Kusumi et al., 1986; Ho & Stubbs, 1992). The problem with this technique is that the probe moiety that senses the solvent environment is so large that spatial resolution may be sacrificed.

(4) Finally, an ESR spin-labeling method has been used in which a nitroxide free-radical moiety is placed at different depths in the lipid bilayer (Griffith et al., 1974; Griffith & Jost, 1976; Kusumi et al., 1986). This method is based on the dependence of unpaired electron spin density at the nitrogen nucleus on solvent polarity. Polar solvents tend to increase the unpaired electron spin density at the nitrogen atom and, therefore, to affect hyperfine interaction between the unpaired electron spin and the nitrogen nuclear spin. In this report, the z component of the hyperfine interaction is referred to as A_z, while one-third of the trace of the tensor (isotropic hyperfine constant) is referred to as A_0. With an increase in solvent polarity, both A_z and A_0 increase. In fact, when Griffith et al. (1974) developed this method, they were the first to describe the shapes of hydrophobicity profiles across lipid bilayer membranes. Using A_z as a convenient experimental observable, water accessibility into the membrane (hydrophobicity profile) was estimated. This clearly demonstrated the presence of the hydrophobic barrier and its approximate shape.

In the present study, we employed the spin-labeling method developed by Griffith et al. (1974) because of its high sensitivity to the changes in hydrophobicity. However, there are four problems associated with this technique. (1) The use of spin probes might perturb the membrane structure. This will be discussed later. (2) Two major types of interactions exist between the N–O group of the nitroxide and the surrounding atoms; van der Waals interaction and hydrogen bonding with water and alcohols, and to a lesser degree with primary and secondary amides. Both interactions significantly influence A_0 and A_z (Griffith et al., 1974; Johnson, 1981). Therefore, the (local) absolute concentration of water near the nitroxide cannot be determined (Griffith et al., 1974). (3) Such measurements must be performed in a frozen suspension of liposomes at −150 °C. This is necessary to distinguish between the motional and solvent effects on the spectrum. At this temperature, no appreciable molecular motion is detected at a time scale of 10^{-7} s. The magnetic parameters (including hyperfine interaction tensors) of spin labels in the membrane determined at lower temperatures have been shown to correlate well with those at physiological temperatures (Kusumi & Pasenkiewicz-Gierula, 1988). In addition, we also examined accessibility of an ion into various parts of the membrane at a physiological temperature and observed a good correlation with the data obtained at lower temperatures. Another issue about lowering temperature is induction of phase separation of cholesterol-rich and cholesterol-poor domains in the presence of cholesterol (up to 50 mol % in this study). As described later, A_z values observed may be weighted averages of the two components whenever cholesterol is present in the membrane. These problems will be further discussed in more detail later in this report. (4) Although spatial resolution is excellent in the frozen solution (gel phase) due to the immobility of the alkyl chains (and localization of most spin density in the nitroxide moiety as compared with the fluorescent probes) (Kusumi et al., 1986), spatial resolution is worse in the liquid-crystalline phase due to the mobility of alkyl chains (Merkle et al., 1987; Ellena et al., 1988). The hydrophobicity profiles across the membrane thus reflect those in the gel-phase well, but they have to be rescaled to take alkyl chain mobility into account in the liquid-crystalline phase.

We use the terms "hydrophobicity" and "polarity" in this report to indicate the solvent effects on hyperfine interaction (Windle, 1981). Qualitatively, A_z is correlated to the concentration of water at a given depth in the membrane, although it does not give the absolute concentration of water. We relate A_z values in the membrane to those in the bulk solvent, by which approximate ϵ (static dielectric constant) at selected depths in the membrane can be estimated.

We have previously investigated the 3-dimensional dynamic structures and molecular miscibilities in PC–cholesterol membranes in the liquid-crystalline phase by varying alkyl chain length, unsaturation, and cholesterol mole fraction. The major results that are relevant to the present study are summarized here. (1) Mismatch in hydrophobic length between the alkyl chains and cholesterol, particularly regarding the bulky tetracyclic ring structure of cholesterol, creates free volume in the central part of the bilayer (cholesterol is usually shorter). (2) Inclusion of a double bond in an alkyl chain, whether it is a *cis* or a *trans* double bond, decreases oxygen transport (the product of the local concentration and the local diffusion coefficient of oxygen) *at all locations* in the membrane. (3) In membranes consisting of *cis*-unsaturated-PC and cholesterol, due to the steric nonconformability between the fused ring structure of cholesterol and the rigid 30° bend at the *cis* double bond in the unsaturated alkyl chains (lateral mismatch in surface topography of two molecules placed side by side in the membrane), the formation of free volume in the membrane center described above is enhanced, and microimmiscibility of *cis*-unsaturated-PC and cholesterol is induced. The cholesterol-rich (or aggregated cholesterol) domains are small (several lipids) and/or of short lifetimes (10^{-9} s to 10^{-7} s) (Kusumi et al., 1986; Kusumi & Pasenkiewicz-Gierula, 1988; Pasenkiewicz-Gierula et al., 1990, 1991; Subczynski et al., 1990; 1991).

The hydrophobicity profiles across PC–cholesterol membranes of various compositions obtained in this work indicate that incorporation of alkyl chain unsaturation and/or cholesterol in the membrane creates effective hydrophobic barriers in the membrane. The detailed profiles of these hydrophobic barriers may provide a basis for understanding membrane permeability to both polar and nonpolar molecules. In addition, such information is necessary for the study of lateral transport and chemical reactions involving small molecules within the membrane. Furthermore, by using water molecules

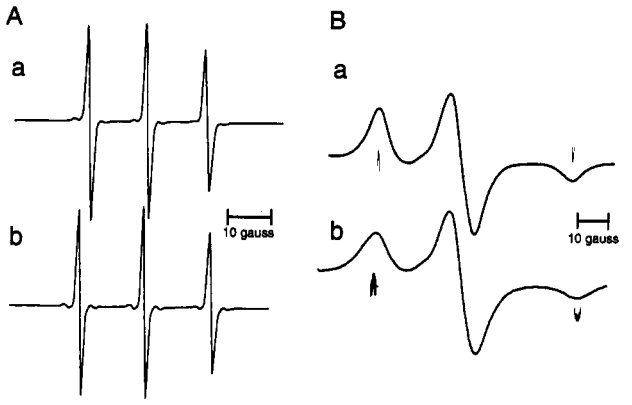

FIGURE 1: (A) X-band ESR spectra of 16-SASL in *n*-hexane (a) and water (b) measured at 25 °C, showing the dependence of A_0 on solvent polarity. A_0 values in the bulk solvents are approximately the same for all SASLs. (B) X-band ESR spectra for 16-SASL in DPPC membranes containing 0 (b) and 30 mol % (a) cholesterol measured at −150 °C, showing the dependence of A_z on the host membrane.

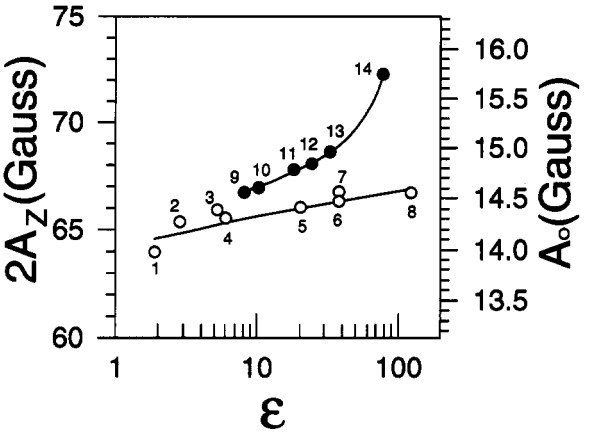

FIGURE 2: $2A_z$ and A_0 for 16-SASL plotted against the dielectric constant ϵ of the solvent at room temperature. The solvents are numbered as follows: (1) hexane, (2) dipropylamine, (3) *N*-butylamine, (4) ethyl acetate, (5) acetone, (6) dimethylformamide, (7) acetonitrile, (8) methylpropionamide, (9) 1-decanol, (10) 1-octanol, (11) 2-propanol, (12) ethanol, (13) methanol, and (14) water. ESR spectra were recorded at 25 °C. See the text for details.

as probes, we observed that cholesterol had dramatic effects on the three-dimensional membrane structure.

EXPERIMENTAL PROCEDURES

Materials. The following reagents were purchased from the indicated sources: all PCs from Sigma; cholesterol (crystallized) from Boehringer Mannheim; stearic acid spin labels (SASL), cholestane spin label (CSL), and androstane spin label (ASL) from Molecular Probes (Eugene, OR), and all organic solvents from Aldrich (Milwaukee, WI). Tempocholine dipalmitoylphosphatidic acid ester (T-PC) was a generous gift from Dr. S. Ohnishi (Kyoto University, Japan). The buffer used was 0.1 M sodium borate at a pH of 9.5. This high pH value ensures that all carboxyl groups of the stearic acid spin labels are ionized in PC membranes (Sanson et al., 1976; Egret-Charlier et al., 1978; Kusumi et al., 1982a,b). In addition, this pH does not alter the structure of PC membranes (Träuble & Eible, 1974; Kusumi et al., 1982a, 1986).

Membrane Preparation and ESR Measurements. The membranes used in this work were multilamellar dispersions of lipids containing 1 mol % of spin label and were prepared as described by Kusumi et al. (1982b, 1986). The lipid dispersion (10^{-5} mol of total lipid/mL) was centrifuged briefly, and the loose pellet (≈20% lipid w/w) was used for ESR measurement. The sample was placed in a 0.9-mm-i.d. gas-permeable capillary made of the methylpentene polymer TPX (Hyde & Subczynski, 1989). The capillary was placed inside the ESR dewar insert and equilibrated with nitrogen gas, which was used for temperature control. The sample was thoroughly deoxygenated at a temperature well above the phase transition of the lipid bilayer. The sample was then frozen (−150 °C), and ESR spectra were obtained at X-band. A Varian E-109 spectrometer with Varian temperature control accessories and an E-231 Varian multipurpose cavity (rectangular TE_{102} mode) was used. For standard ESR spectroscopy, the temperature was monitored using a copper–constantan thermocouple that was placed in the sample just above the active volume of the cavity. ESR spectra for bulk solvents were recorded at 25 °C.

The short-pulse saturation recovery ESR experiments were performed for dioleoyl-PC (DOPC) membranes as described previously (Yin et al., 1987; Subczynski et al., 1990, 1991). To avoid artificial shortening in T_1 measurement, a relatively low level of observation power (8 μW, with the loop-gap resonator delivering an H_1 field of 3.6×10^{-5} G) was used for all experiments. All saturation recovery decays were measured on the central line. Under the experimental conditions employed here, all recovery curves could be fitted to one-component exponential recovery curves.

RESULTS AND DISCUSSION

Solvent Dependence of ESR Spectra for SASLs. Chart 1 shows the chemical structures of spin labels used in this work. To indicate the approximate location of the nitroxide group in the membrane, the chemical structures of L-α-dimyristoylphosphatidylcholine (DMPC) and cholesterol are also shown, and they are all arranged according to the orientation and location in the membrane (7-, 9-, 10-, 12-SASLs are not shown).

Figure 1A shows ESR spectra for 16-SASL solubilized in hexane and water at 25 °C, while Figure 1B shows those in L-α-dipalmitoylphosphatidylcholine (DPPC) membranes in the presence and absence of 30 mol % cholesterol at −150 °C. These figures indicate that both A_0 obtained in solution at 25 °C and A_z (*z* component of the hyperfine interaction tensor) determined in the membrane at −150 °C are sensitive to changes in the polarity of the environment (Cohen & Hoffman, 1973; Griffith et al., 1974; Pasenkiewicz-Gierula et al., 1983; Kusumi & Pasenkiewicz-Gierula, 1988). The changes in A_z with changes in polarity are much greater than those in A_0 (Kusumi & Pasenkiewicz-Gierula, 1988). Since $2A_z$ can be determined directly from the ESR spectra of the frozen samples, as illustrated in Figure 1B, we employed $2A_z$ as a parameter of the extent of water penetration into the membrane. All measurements of $2A_z$ were carried out at −150 °C since $2A_z$ does not depend on temperature below −140 °C (Johnson, 1981; Kusumi & Pasenkiewicz-Gierula, 1988).

In this work, we relate local hydrophobicity as observed by $2A_z$ at a selected depth in the membrane to hydrophobicity (or ϵ) of bulk organic solvents. This approach was based on two previous findings.

(1) A_z in frozen solution can be related to A_0 in liquid solution, because A_0 values determined in the bulk solution before and after freezing are similar (Griffith et al., 1974;

Chart 1

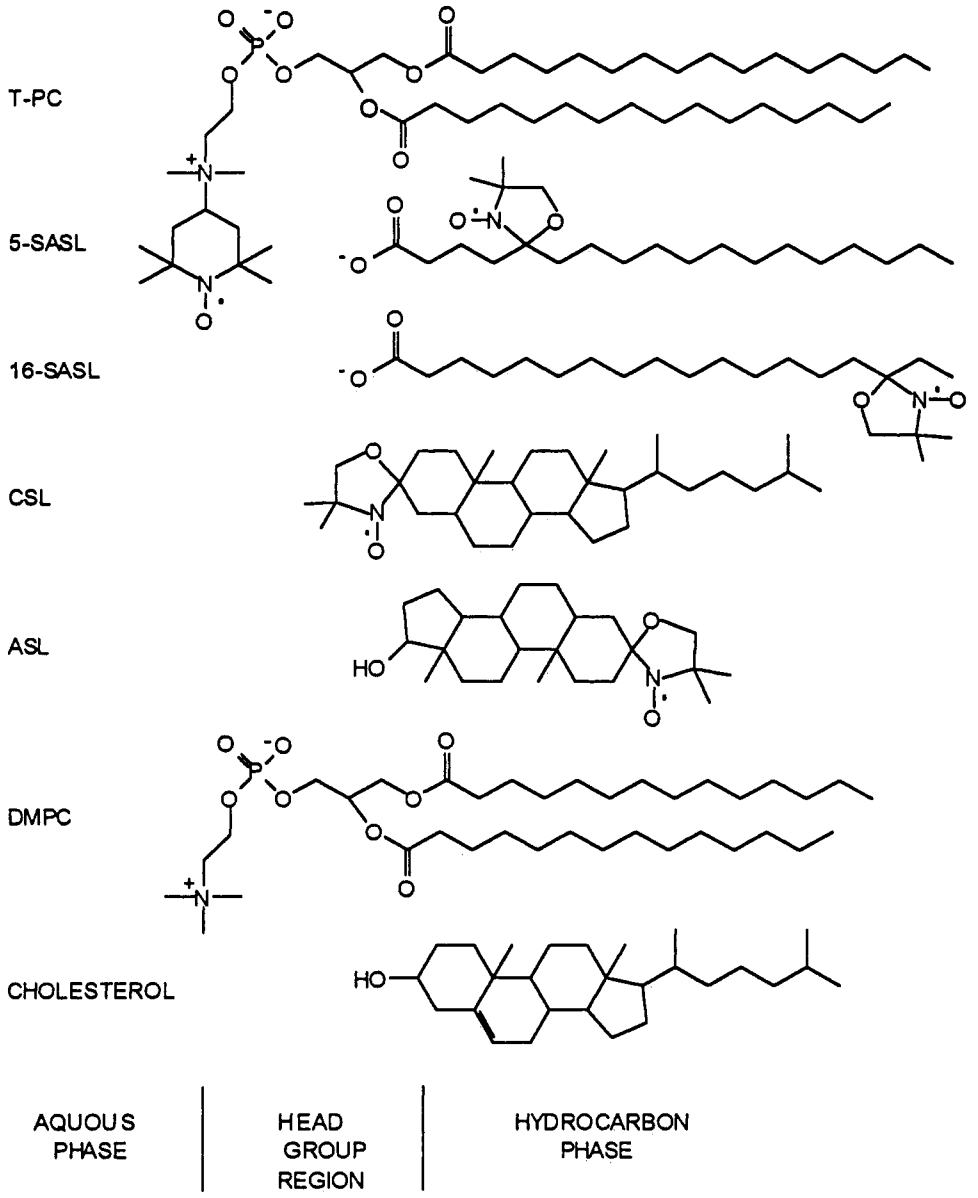

Johnson, 1981; Pasenkiewicz-Gierula et al., 1983). A relationship was experimentally determined for SASL by measuring both parameters in various solvents,

$$A_0(\text{liquid}) = aA_z(\text{frozen}) + b \qquad (1)$$

where $a = 0.426$ and $b = 0.349$ G when A_0 and A_z are expressed in Gauss (Griffith et al., 1974; also confirmed by us). Similar relationships between A_0 and A_z have been reported for other spin labels (Lassmann, et al., 1973; Cohen & Hoffman, 1973). Therefore, assuming that A_z determined in the frozen membrane can be related to A_z in the frozen solution of a bulk solvent, A_z of the frozen membrane can in turn be related to A_0 in the bulk liquid solvent.

(2) Griffith et al. (1974) found a good correlation between A_0 for di-*tert*-butyl nitroxide dissolved in organic solvents and the static dielectric constants of the solvents. In the plot of A_0 versus $(\epsilon-1)/(\epsilon+1)$, where ϵ is the static dielectric constant of the solvent at room temperature, two curves (such as those shown in Figure 2) were obtained that are close to each other yet distinct. The points for solvents that can form hydrogen bonds with the N–O group fell near one curve, and those for solvents that cannot fell near the other curve.

In the present study, similar measurements were carried out using 16-SASL in various solvents. The observed A_0 values are plotted as a function of ϵ (Figure 2). Other SASLs showed similar values (data not shown). The ordinate scale in Figure 2 also indicates $2A_z$, calculated by using eq 1. Hydrophobicity at a given depth in the membrane parametrized with $2A_z$ can be related to that of a bulk organic solvent by referring to Figure 2. The difference between the solvents that can and cannot form hydrogen bonds with the N–O group is clear in Figure 2. We used the curve for the *hydrogen bond-forming solvent* (upper curve), except for cases in which the local membrane hydrophobicity is high, because water plays a key role in determining $2A_z$. $2A_z$ in the bulk solvent provides a convenient yardstick for describing local hydrophobicity in the membrane, and comparison of two $2A_z$ values may help to develop a "feel" for local hydrophobicity. Such a comparison is only semiquantitative and could be done operationally because small changes in $2A_z$ correspond to large changes in ϵ and because the mechanism by which the presence of water affects $2A_z$ is not well understood. Nevertheless, since this comparison is made for systematic measurements for both the membrane systems and various bulk solvents (also note

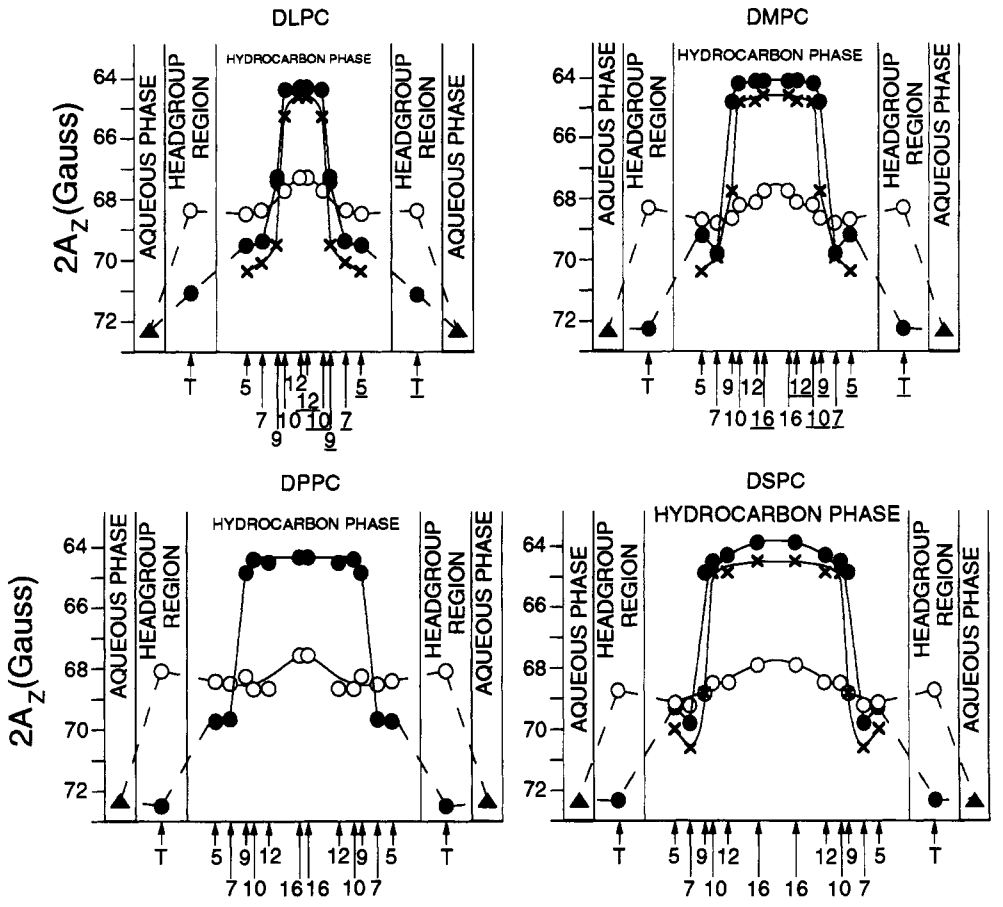

FIGURE 3: Hydrophobicity profiles ($2A_z$) across saturated-PC membranes and those containing 30 and 50 mol % cholesterol. Upward changes indicate increases in hydrophobicity. The data for DLPC, DMPC, DPPC, and DSPC membranes are shown. Approximate locations of the nitroxide moieties of spin labels are indicated by arrows under the base line. The underlined numbers for *n*-SASL for DLPC and DMPC indicate that these SASLs are intercalated mainly in the right half of the bilayer. (SASLs are longer than most of the host phospholipids.) T indicates T-PC. Symbols: 0 (○), 30 (●), and 50 (×) mol% cholesterol. $2A_z$ for SASL in the aqueous phase was calculated from A_0 (Figure 2) using eq 1. Broken lines are used for connecting the points obtained with different types of the nitroxide radicals.

that most comparisons were made for hydrogen-bonding solvents), we believe that such a comparison is useful if it is done with care. Readers are warned not to overinterpret it.

The cholesterol mole fraction examined in this work is in the range of 0–50%. Within this range, phase separation of cholesterol-rich and cholesterol-poor domains is expected to occur (Subczynski et al., 1991). Although we did not observe any indication of the presence of two components in any ESR spectrum, the spectra, thus $2A_z$ values, may be weighted averages of the two components whenever cholesterol is present in the membrane.

Hydrophobicity Profiles of Saturated-PC Membranes: Effect of Alkyl Chain Length. A_z values were measured from the ESR spectra for *n*-doxylstearic acid spin labels (*n*-SASLs, where $n = 5, 7, 9, 10, 12$, and 16), with their nitroxide groups placed at various depths in the membrane. In addition, tempocholine dipalmitoylphosphatidic acid ester (T-PC) and cholestane spin label (CSL) were used to probe the membrane surface, while androstane spin label (ASL) was used to monitor hydrophobicity in the interior region of the membrane. CSL and ASL also serve to mimic the behavior of cholesterol, thus probing hydrophobicity around cholesterol molecules in the surface and interior regions, respectively. To study the effect of alkyl chain length on hydrophobicity profiles across the bilayer, PC bilayers consisting of dilauroyl-, dimyristoyl-, dipalmitoyl, and distearoyl-PC (DLPC, DMPC, DPPC, and DSPC, respectively) were investigated.

Figure 3 shows the hydrophobicity profiles across these membranes. In such figures, $2A_z$ data are presented as a function of the approximate position of the nitroxide moiety of the spin label within the lipid bilayer (the width of the hydrocarbon phase and the locations of the spin probe in the stearic acid are simply scaled to the number of carbon atoms in the alkyl chain). Smaller $2A_z$ values (upward changes in the profiles) indicate higher hydrophobicity. The hydrophobicity profiles show gradual increases toward the bilayer center for all saturated-PC membranes. However, the changes are small in the absence of cholesterol. Longer alkyl chains simply make the central hydrophobic regions wider without increasing hydrophobicity at the bilayer center. In fact, all of the membranes investigated here have similar $2A_z$ values at the membrane center and in the polar headgroup region.

An unexpected finding is that even at the center of the membrane, the saturated-PC membranes are not as hydrophobic as one might have expected. Hydrophobicity at the membrane center is close to those of 2-propanol and 1-octanol, which have dielectric constants of 10–20 (cf. Figure 2). This result is, in fact, consistent with a classical paper by Diamond and Katz (1974), who concluded that the average environment around small nonelectrolytes dissolved in the membrane is slightly less hydrophobic than 1-octanol and similar to 1-pentanol. In contrast, these results are at variance with the dielectric constants of 2–2.2 which are often used to estimate membrane thickness from measurements of membrane capacitance (Ohki, 1969; Simon et al., 1982).

Effects of Cholesterol on Hydrophobicity Profiles in Saturated-PC Membranes. Cholesterol has dramatic effects

on the hydrophobicity profiles of saturated-PC membranes. Hydrophobicity profiles in the presence of 30 and 50 mol % cholesterol in saturated-PC membranes with various alkyl chain lengths are illustrated in Figure 3. Four remarkable features of the effects of cholesterol are noted.

(1) The Presence of cholesterol induces an increase in polarity in both the polar headgroup region and the hydrocarbon region up to the depth of the seventh carbon.

(2) The presence of cholesterol also causes a considerable increase in hydrophobicity in the central region of the bilayer, which is deeper than the ninth carbon. Hydrophobicity reaches the level of hexane. These results (1 and 2) agree with our previous observation using CSL (for frozen samples) and fluorescent probes (for membranes in the liquid-crystalline phase) (Kusumi et al., 1986). Incorporation of cholesterol in saturated PC is likely to separate the headgroups in the polar region and to induce packing defects in the regions where alkyl chains and the bulky, rigid steroid ring structure are apposed side by side, thereby creating free space from the glycerol backbone region to the seventh carbon in the acyl chain through which water molecules enter.

(3) The profiles show sharp increases in hydrophobicity between the seventh and ninth carbons at 30 mol % cholesterol for DMPC, DPPC, and DSPC membranes. This sharp transition point shifts toward inside the membrane as the cholesterol content is increased to 50 mol %. The transition point for DLPC–cholesterol membranes shifts slightly inward, between the seventh and tenth positions, and the transition is not as sharp as those of the other membranes. Since alkyl chains in DLPC are shorter than those in cholesterol and SASL, the behavior of DLPC membrane is usually slightly different than those of other saturated-PC membranes (Kusumi et al., 1986).

(4) The $2A_z$ values are almost constant (within a gauss) inside the sharp transition points in the profiles. In addition, the $2A_z$ values in the presence of 30 mol % cholesterol are almost the same for all saturated-PC membranes. A further increase in the cholesterol content causes slight *decreases* in $2A_z$.

These results are somewhat different than those of Hiff and Kevan (1989), who studied the effect of 20 mol % cholesterol on DL-α-DPPC membranes in frozen solution at 77 K. They observed electron spin echo modulation signals of SASLs, which were induced through interaction of the nitroxide with D_2O (used instead of H_2O as a modulator). They observed a cholesterol-induced increase in water penetration in the polar headgroup region and up to the position of 10-SASL in the hydrocarbon phase but little cholesterol-induced changes in the inner regions. This observation was carried out in unilamellar small liposomes made of DL-form DPPC which were prepared by sonication. The pH used was 7.0, at which both protonated and unprotonated forms of SASLs are present in the membrane. These forms of SASLs are located at different depths in the membrane and give different ESR signals (Egret-Charlier et al., 1978; Kusumi et al., 1982a,b).

Hydrophobicity Profiles of Unsaturated-PC Membranes: Effects of Cis and Trans Double Bonds at C9–C10. To investigate the effect of introducing a double bond into the alkyl chain, we compared the hydrophobicity profile of DSPC (a saturated PC) membranes with those of L-α-dioleoyl-PC (DOPC) and L-α-dielaidoyl-PC (DEPC) membranes. These lipids all contain 18 carbons per alkyl chain and differ only in terms of unsaturation. DEPC contains a C9–C10 *trans* double bond, while DOPC has a C9–C10 *cis* double bond in each alkyl chain. As a model of biological membranes with mixed alkyl chains, bilayer membranes made of egg-yolk PC (EYPC) were also studied.

The hydrophobicity profiles of these membranes are shown in Figure 4. Introduction of unsaturation into hydrocarbon chains changes the shape of the hydrophobicity profiles. The double bond *increases* hydrophobicity *at all locations* in the membrane. The increase induced by the *cis* double bond (DOPC) is greater than that induced by the *trans* bond (DEPC) and is close to that induced by incorporation of 30 mol % cholesterol. The hydrophobicity reaches approximately that of dipropylamine. These results suggest that water penetration into the hydrocarbon phase in the membrane is strongly suppressed by the presence of a *cis* double bond in the alkyl chain. The smaller effect of the *trans* double bond may be explained by the conformational similarity of elaidoyl chains to saturated chains with the *trans* conformation.

The hydrophobicity profile of EYPC membranes lies between those of DEPC and DOPC membranes, probably because EYPC is a mixture of PCs which contain both saturated and unsaturated alkyl chains. Approximately 70% of EYPC is 1-palmitoyl-2-oeloyl-PC (Seelig & Waespa-Sarcevic, 1978). $2A_z$ in the central part of the bilayer is similar to that in DOPC membranes.

These results agree with the fact that saturated hydrocarbons are much more hygroscopic than unsaturated hydrocarbons. Hiff and Kevan (1989), using electron spin echo modulation measurements in frozen liposome suspension, also showed that water accessibility to the *n*-SASL's nitroxide depends on lipid unsaturation in the order DL-DPPC $\approx$ DEPC $\gg$ DOPC (no water was detected in the hydrocarbon phase of DOPC). It appears that observing the interaction between the nitroxide and D_2O by electron spin echo modulation is less sensitive than the method employed here when the water concentration is low.

Effects of Cholesterol on Hydrophobicity Profiles of Unsaturated-PC Membranes. The effects of 30 and 50 mol % cholesterol on the hydrophobicity profiles of unsaturated-PC membranes are shown in Figure 4. The hydrophobicity profile for the DEPC–30 mol % cholesterol membrane is similar to that for the DSPC–30 mol % cholesterol membrane. The increase in cholesterol-enhanced hydrophobicity in the central part of the DEPC membranes is smaller than those in saturated-PC membranes because the DEPC membrane itself already possesses higher hydrophobicity than the DSPC membrane.

The effect of cholesterol on DOPC membranes has three characteristic features.

(1) The cholesterol-induced increase in $2A_z$ in the polar headgroup region (T-PC) is smaller than those for DSPC and DEPC membranes.

(2) A large cholesterol-induced decrease in hydrophobicity in the vicinity of 5- and 7-SASL was observed in DOPC–cholesterol membranes. Since DOPC membranes in the absence of cholesterol at these positions show greater hydrophobicity than DSPC membranes without cholesterol, the cholesterol-induced decrease in hydrophobicity of DOPC–cholesterol membranes near the 5- and 7-positions is particularly marked. As discussed in the previous section, such decreases in hydrophobicity are thought to be induced by the packing defects generated by intercalation of the steroid ring structure. Water molecules enter the free volume created by the packing defects. The tendency for formation of such defects may be larger in DOPC membranes because of the steric nonconformability between the rigid bulky steroid ring

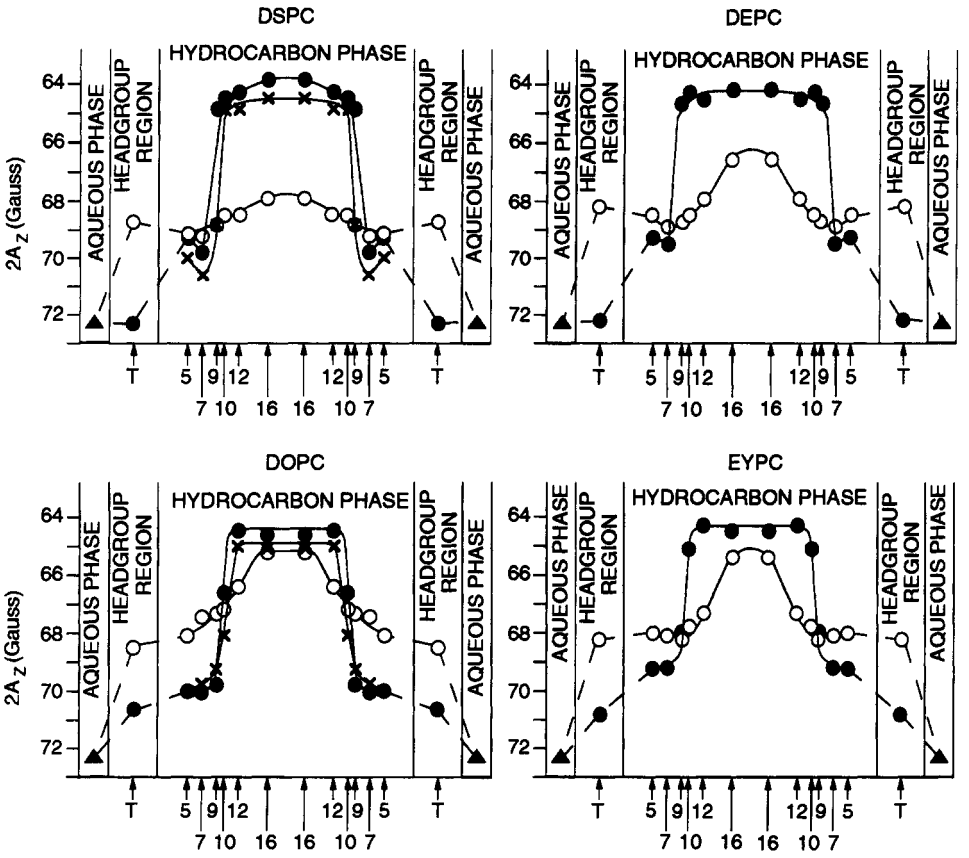

FIGURE 4: Hydrophobicity profiles ($2A_z$) across unsaturated-PC membranes containing 18 carbons per alkyl chain. The effects of incorporation of 30 and 50 mol % cholesterol are also shown. Upward changes indicate increases in hydrophobicity. The data for DEPC, DOPC, and EYPC membranes are displayed as well as those for DSPC membrane as a control. The symbols are the same as those used in Figure 3.

structure and the rigid 30° bend of oleoyl chains at the C9 position (Subczynski et al., 1990, 1991), which thereby induces greater water penetration.

(3) In DSPC–cholesterol membranes, sharp increases in hydrophobicity occur between the seventh and ninth carbons with 30 mol % cholesterol and between ninth and tenth carbons with 50 mol % cholesterol. In contrast, in DOPC–cholesterol membranes, sharp cholesterol-induced increases occur between the ninth and tenth carbons with 30 mol % cholesterol and between the 10th and 12th carbons with 50 mol % cholesterol.

(4) The level of hydrophobicity in the middle of the DOPC–cholesterol membrane is approximately the same as that for other membranes in the presence of cholesterol, which is about the level of bulk hexane. Since the level of hydrophobicity in the middle of the bilayer in the DOPC membrane is already at about this level, the cholesterol-induced increment in the central region is much smaller.

In the case of EYPC–cholesterol membranes, the cholesterol-induced changes lie between those in DEPC and DOPC membranes.

Taken together, the presence of more than 30 mol % cholesterol in the membrane makes the profiles trapezoidal in the hydrocarbon phase, with a very sharp increase within one or two carbons in the region of C7 or C12 (depending on the membrane). This level of cholesterol produces gradual changes in the hydrophobicity profiles between the aqueous phase and the near-surface region in the hydrocarbon phase. The presence of cholesterol increases hydrophobicity in the middle of the bilayer from the levels of 2-propanol or 1-octanol (saturated PCs), ethyl acetate or dimethylformamide (DEPC), and dipropylamine (DOPC) to the level of hexane (for all PCs in the presence of cholesterol).

Griffith et al. (1974) compared $2A_z$ values for microsomal membranes and those for myelin membranes using 5-, 12-, and 16-SASL. $2A_z$ for 5-SASL in myelin membranes indicate lower hydrophobicity than that in microsomal membranes, while those for 12- and 16-SASL indicate higher hydrophobicity in myelin membranes. These results agree with the present data because myelin membranes contain a higher level of cholesterol than microsomal membranes.

Many studies have been performed on the depth of water penetration or effective membrane thickness using the capacitance measurement of planar black lipid membrane. In these studies, the effective membrane thickness was calculated from the measured capacitance by assuming a dielectric constant which is almost always in the range of 2–2.2 [for example, Ohki (1968), Fettiplace et al. (1971), Simon et al. (1982)]. According to the present results, this value is only realized in the presence of cholesterol. The full width at half-height of the trapezoidal profile in the central part of the membrane containing 30 mol % cholesterol (the points at which these widths are determined gives $2A_z \approx 67$ G, corresponding to dielectric constants between 9 and 19, which are similar to those for acetonitrile and 1-decanol) is about 50% of the thickness of the hydrocarbon phase, approximately 1.5–2 nm. The thickness obtained from capacitance measurements is ≈3 nm. (We suspect that, due to the residual solvents used to form the black membrane, the membrane capacitance is also underestimated, thereby apparently reducing the error of the estimate).

Simon et al. (1982) concluded that the effective thickness ("dielectric thickness") increases in the presence of cholesterol in bacterial PE membranes from 2.82 nm in the absence of cholesterol to 3.09 and 3.42 nm in the presence of 30 and 50

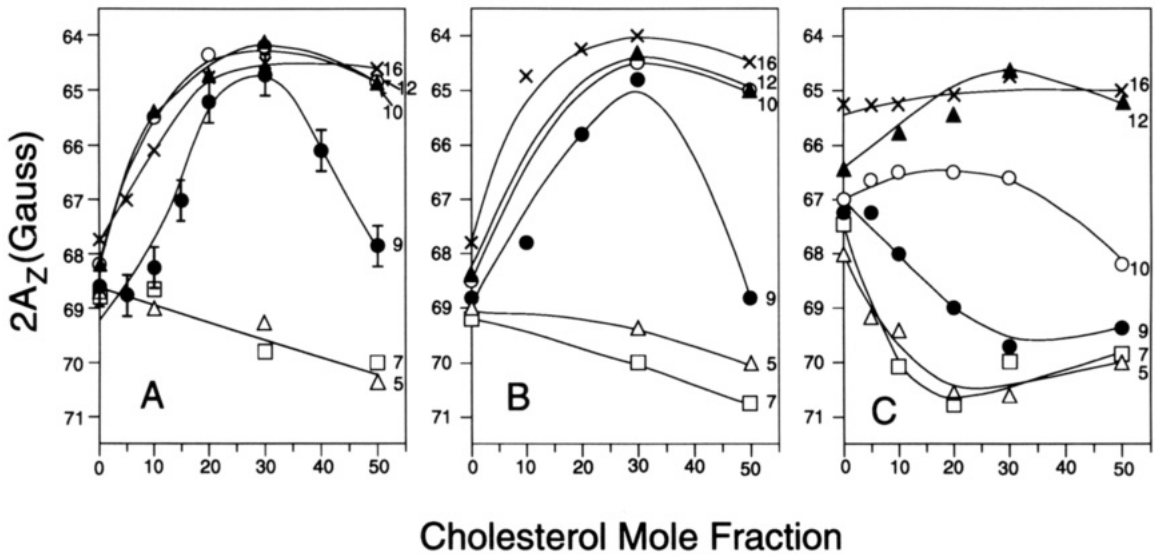

FIGURE 5: $2A_z$ values for various *n*-SASLs plotted as a function of cholesterol mole fraction. Upward changes indicate increases in hydrophobicity. (A) DMPC, (B) DSPC, and (C) DOPC. Numbers indicate *n* for *n*-SASL.

mol % cholesterol, respectively, on the basis of specific capacitance measurement. This conclusion was obtained by assuming that the dielectric constant in the membrane core region is 2.2 regardless of the cholesterol contents in the membrane. The experiments by Diamond and Katz (1974) and those presented here clearly show that such an assumption is invalid.

Thus, one of the most important conclusions obtained in the present study is that the extent of water penetration into the membrane is much higher than that previously assumed by many researchers. The hydrophobic barriers of saturated-PC membranes are low. Unsaturation of alkyl chains and/or addition of cholesterol decreases the extent of water penetration into the core region of the bilayer, but the thickness of the region that is relatively protected from water penetration is about half of the physical thickness of the hydrocarbon phase, even in the presence of 30–50 mol % cholesterol.

Dependence of Membrane Hydrophobicity on Cholesterol Contents. The dependence of local membrane hydrophobicity as observed with *n*-SASLs upon cholesterol concentration in DMPC, DSPC, and DOPC membranes is illustrated in Figure 5 in more detail. In each membrane, cholesterol intercalation has the distinguished effect between two membrane regions with different depth: one in which hydrophobicity decreases with an increase in the cholesterol mole fraction from 0 to 30 mol %, and the other in which hydrophobicity decreases with an initial increase in the cholesterol mole fraction. In DMPC and DSPC membranes (Figure 5A and B, respectively), the local hydrophobicity monitored with 5- and 7-SASL decreases, and that monitored with 9-, 10-, 12-, and 16-SASL increases with an increase in the cholesterol mole fraction. In contrast, in DOPC membranes, the local hydrophobicity monitored with 5-, 7-, and 9-SASL decreases, and that monitored with 12- and 16-SASL increases, while 10-SASL shows little changes (up to 30 mol % cholesterol).

The *n*-SASLs that show an initial increase in local hydrophobicity with an increase in the cholesterol concentration also show decreases when the cholesterol mole fraction is increased from 30 to 50 mol %. This tendency is particularly marked in saturated-PC membranes and with 9-SASL. From Figures 3, 4, and 5, it is clear that the widths of the high-hydrophobic plateaus decrease as cholesterol concentration is increased from 30 to 50 mol %, which suggests that membrane thickness decreases. This may be due to tail-to-tail apposition

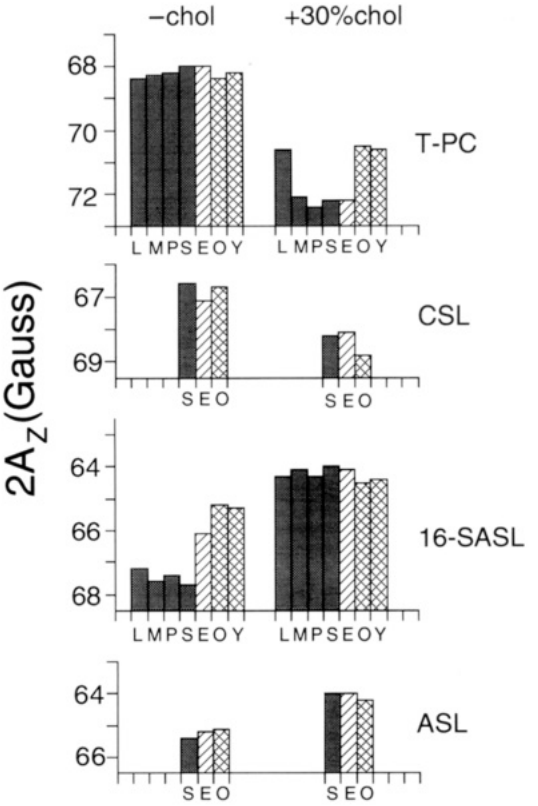

FIGURE 6: $2A_z$ values (in gauss) are shown for membranes without cholesterol (left column) and with 30 mol % cholesterol (right column) measured with T-PC, CSL, 16-SASL, and ASL. Taller bars indicate higher hydrophobicity. Note that the absolute scales for $2A_z$ are different for each row to save space. T-PC and CSL are probes for the near-surface region of the membrane, while 16-SASL and ASL are probes for the center of the membrane. ASL and CSL are cholesterol-like probes. Symbols: L, DLPC; M, DMPC; P, DPPC; S, DSPC; E, DEPC; O, DOPC; Y, EYPC; dark bars, PCs with saturated alkyl chains; hatched bars, PC with *trans* unsaturation (DEPC); cross-hatched bars, PC with *cis* unsaturation (DOPC and EYPC).

of cholesterol from both sides of the membrane with these high concentrations of cholesterol.

Figure 6 summarizes the effect of 30 mol % cholesterol on a variety of PC membranes at the membrane surface and in the middle of the bilayer, as probed by T-PC and CSL and

by 16-SASL and ASL, respectively. CSL and ASL are cholesterol analog spin labels. The nitroxide moiety of CSL is located at about the level of the PC glycerol backbone, while that of ASL is located near C12 of PC in the membrane, near the end of the sterol ring of cholesterol (Subczynski et al., 1990, 1991).

Both T-PC and CSL indicate that cholesterol decreases hydrophobicity near the membrane surface. Observation with T-PC indicates that the extent of the cholesterol effect is smaller in DOPC and EYPC membranes than in saturated-PC and DEPC membranes (except for DLPC membranes); since the alkyl chains are shorter than those in cholesterol, the behavior of DLPC membrane with cholesterol incorporation is often somewhat different from those of other saturated-PC membranes), but CSL observation indicates that the effect is about the same for all PC membranes.

16-SASL indicates that the membrane central region is more hydrophobic in unsaturated-PC membranes than in saturated-PC membranes. However, ASL shows only slight differences in hydrophobicity in the presence of double bonds (compare S, E, O in the –chol column in Figure 6 with 16-SASL and ASL). In the presence of 30 mol % cholesterol, both 16-SASL and ASL show a similar level of hydrophobicity in all of the membranes. Although such differences between PC analog and cholesterol analog spin labels are small, they suggest the presence of PC–cholesterol immiscibility in PC–cholesterol membranes.

Effects of Cholesterol on Ion Penetration into the Membrane. Since the above measurements were all performed at −150 °C, these results were compared with the level of ion penetration into the membrane under physiological conditions. We investigated the magnetic interaction of $Fe(CN)_6^{3-}$ dissolved in water with SASLs in the membrane by measuring the spin–lattice relaxation times (T_1) of spin labels. Bimolecular collision of $Fe(CN)_6^{3-}$ (a fast-relaxing species) with nitroxide (a slow-relaxing species) induces spin exchange, which leads to a faster effective spin–lattice relaxation of the spin labels (Molin et al., 1980). The collision rate should then reflect the degree of penetration of $Fe(CN)_6^{3-}$ into the lipid bilayer. In an analogy to an oxygen transport parameter defined previously (Kusumi et al., 1982b), we used the parameter

$$P(x) = T_1^{-1}(50\ \text{mM}\ K_3Fe(CN)_6; x) - T_1^{-1}(\text{no}\ K_3Fe(CN)_6; x) \quad (2)$$

This parameter is proportional to the product of the local concentration and the local translational diffusion coefficient of $K_3Fe(CN)_6$ at the membrane "depth" x, at which the nitroxide moiety is located. Greater $P(x)$ values indicate a greater extent of $K_3Fe(CN)_6$ penetration into the membrane.

Typical saturation recovery curves of 9-SASL in DOPC–30 mol % cholesterol membrane *in the fluid phase* in the presence and absence of 50 mM $K_3Fe(CN)_6$ are shown in Figure 7. T_1 was measured with an accuracy better than 5%. Figure 7 shows that the collision of $K_3Fe(CN)_6$ with the spin label decreases T_1 of the nitroxide.

Saturation recovery measurements were carried out for various SASLs in DOPC membranes at 25 °C in the presence and absence of 30 mol % cholesterol and 50 mM $K_3Fe(CN)_6$, and $P(x)$ values are shown in Figure 8 as a function of the location of nitroxide in the stearic chain. In the absence of fast-relaxing iron ions, incorporation of cholesterol only slightly affects T_1 (Subczynski et al., 1989, 1991).

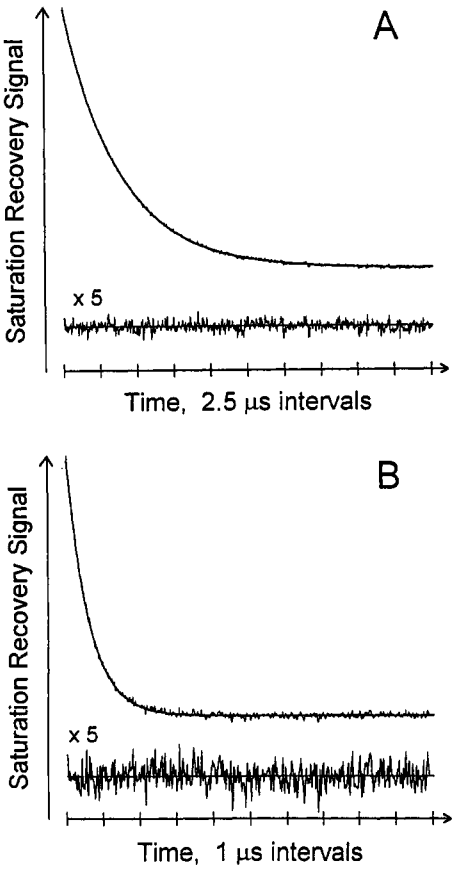

FIGURE 7: Representative saturation recovery ESR curves. 9-SASL in DOPC–30 mol % cholesterol membrane in the absence (A) and presence (B) of 50 mM $K_3Fe(CN)_6$ measured at 25 °C. The experimental and best-fit recovery curves are superimposed. The difference between experimental data and the exponential fit is shown enlarged five times. T_1 is 4.75 and 0.62 μs in the absence and presence of $K_3Fe(CN)_6$, respectively.

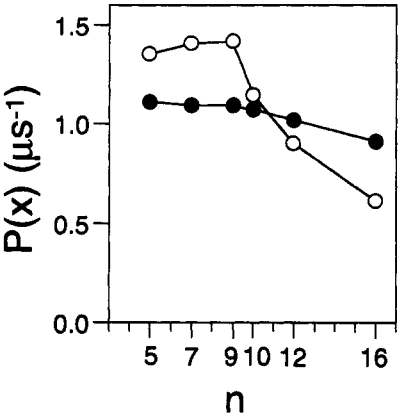

FIGURE 8: $P(x) = T_1^{-1}(50\ \text{mM}\ K_3Fe(CN)_6; x) - T_1^{-1}(\text{no}\ K_3Fe(CN)_6; x)$ plotted as a function of the position of the nitroxide on SASL at 25 °C in DOPC–cholesterol membranes. In the absence of $K_3Fe(CN)_6$, 300 mM NaCl was added instead. Symbols: ●, no cholesterol; ○, with 30 mol % cholesterol.

In the absence of cholesterol, penetration of $K_3Fe(CN)_6$ into DOPC membranes gradually decreases toward the membrane center.

In the presence of 30 mol % cholesterol, the level of penetration of $K_3Fe(CN)_6$ increases up to the depth of the ninth carbon, while it decreases at the 12th and 16th carbons. The presence of cholesterol creates abrupt changes in the accessibility of $K_3Fe(CN)_6$ at the depth of the 10th carbon. These profiles correlate well with those shown in Figure 4 (DOPC).

GENERAL DISCUSSION

Extent of Water Penetration into the Membrane. Hydrophobicity in the membrane is largely determined by the extent of water penetration into the membrane (Griffith et al., 1974). The general shape of the hydrophobicity profile in the absence of cholesterol agrees well with the data obtained by Griffith et al. (1974) for liposomes made of the total lipid extract of microsomes, which does not contain appreciable amounts of cholesterol. Our results also generally agree with the profile obtained by Fretten et al. (1980) for chromaffin granule membranes using A_0 of SALSs at physiological temperatures. They noted no changes in A_0 between 20 and 50 °C. We did not employ their method in this study because the method of A_0 estimation has to be changed for different SASLs, which makes the obtained hydrophobicity profile less reliable. Nevertheless, such agreement shows that the hydrophobicity profiles obtainedat −150 °C provide good estimates of those at physiological temperatures.

Three other pieces of evidence support the validity of hydrophobicity profiles obtained in this work. The first supporting evidence comes from simulation of CSL ESR spectra that were measured for a variety of membranes in the liquid-crystalline phase using magnetic parameters (including all of the tensor components of hyperfine interaction) determined at −120 °C. Successful simulations of ESR spectra taken at physiological temperatures were only possible by using magnetic parameters determined specifically for each membrane with specific host lipids (Kusumi & Pasenkiewicz-Gierula, 1988). The second is that fluorescence spectrum of 12-(9-anthroyloxy)stearic acid shows cholesterol-induced decreases in water accessibility into hydrophobic loci (near 12-SASL) of the DPPC membrane in the fluid-phase at 50 °C (Kusumi et al., 1986). The third is that a good correlation was found between the hydrophobicity profiles and the permeability of small molecules across the membrane, which will be discussed in detail in the next subsection.

Permeability of Small Polar Molecules across the Lipid Bilayer Membrane. (1) Effects of Unsaturation of Alkyl Chains. The present results indicated that the presence of either *trans* or *cis* double bonds *increases* hydrophobicity in the membrane. The effect of a *cis* double bond is much greater than that of a *trans* double bond. These results agree with permeability measurements of small polar molecules across the membrane; permeability of water (Carruthers & Melchior, 1983; Daemer & Bramhall, 1986; Lazrak et al., 1987) and amino acids (glycine, lysine, and serine; Chakrabarti & Daemer, 1992) across unsaturated-PC (DOPC and EYPC) membranes is 1.4–4.2 times less than that across saturated-PC membranes. These results suggest that hydrophobicity profiles provide a basis for understanding the permeability of small polar molecules across the membrane.

The only permeability data which are not consistent with those obtained here regarding the effect of unsaturation on membrane hydrophobicity are those by Carruthers and Melchior (1983). They measured water permeability of DPPC membranes at ≈52 °C, that of DSPC membranes at ≈62 °C, and that of DEPC membranes at ≈24 °C [all ≈10 °C above the main phase transition temperatures]. Although direct comparison of these data may be difficult since these measurements were performed at different temperatures, Carruthers and Melchior reported water permeabilities of (6.32 ± 0.18)-, (2.9 ± 0.3)-, and (7.51 ± 0.29) × 10^{-4} cm/s for DPPC, DSPC, and DEPC membranes, respectively, while we expect lower permeability for DEPC membranes (see Figure 4).

(2) Effects of Cholesterol. Incorporation of 30 mol % cholesterol into DMPC and DPPC membranes decreases water permeability by factors of 3 and 9, respectively (Milon et al., 1986; Carruthers & Melchior, 1983), while that into EYPC membranes reduces water permeability by a factor of between 1.6 and 3.9 (Lazrak et al., 1987; Finkelstein, 1976). The effect of cholesterol on permeability of saturated-PC membranes is in general greater than that on the permeability of unsaturated-PC membranes, which is consistent with the present data. Since water permeability is decreased in the presence of cholesterol, which induces both increases of hydrophobicity in the central part of the membrane and enhancement of water penetration into the near-surface region in the hydrocarbon phase, the rate-limiting step for permeability of small polar molecules is likely to be the process of crossing the hydrophobic barrier at the membrane center.

Carruthers and Melchior (1983) studied the effect of incorporation of cholesterol on water permeability in DMPC membranes. Above 35 °C, increasing the cholesterol content from 0 to 27 mol % induced a monotonic decrease in the permeability of DMPC membranes. A further increase in the cholesterol mole fraction to 50 mol % increased water permeability monotonically. These results correlate well with the dependence of hydrophobicity on cholesterol mole fraction monitored by 9-, 10-, 12-, and 16-SASL, i.e., in the core region of the DMPC bilayer, where the hydrophobic permeability barrier is located (see Figure 5A). These SASLs show increases in hydrophobicity with an increase in cholesterol contents from 0 to 30 mol % and decreases with a further increase in cholesterol. The spatial variation in the extent of water penetration creates the hydrophobicity profile across the membrane, and the profile is likely to determine the energetical ease with which polar molecules including water travel across the membrane.

(3) Hydrophobic Barriers of the Membrane against Permeation of Small Molecules. Permeability coefficients of small nonelectrolytes correlate well with oil/water partition coefficients [Overton's rule (Overton, 1899)]. In discussions of the mechanism by which small nonelectrolytes permeate across model and biological membranes, particular attention has been directed toward (1) the location of the permeation barriers in the lipid bilayer, and (2) the physical nature of the rate-limiting barrier (Diamond & Katz, 1974; Walter & Gutknecht, 1986; Leahy & Wait, 1986; Lieb & Stein, 1986; Subczynski et al., 1992).

We have previously shown that the major resistance to permeation of molecular oxygen across the membrane is located at the polar headgroup region and the near-surface region in the hydrocarbon phase (Subczynski et al., 1989, 1991). These results suggest that the locations of the permeation barriers are different for polar and nonpolar molecules: for polar molecules, the major permeation resistance is the *hydrophobic barrier* in the central part of the membrane, while for nonpolar molecules, the resistance is the *rigidity barrier* near the membrane surface.

Plasma membranes are known to contain large concentrations of cholesterol, while cholesterol concentrations in intracellular membranes are low. The role of cholesterol in the plasma membrane is a long-standing puzzle. It has been proposed that the mixture of saturated and unsaturated alkyl chains with cholesterol provides a fluidity buffer (Kusumi et al., 1983, 1986). The present results suggest that cholesterol has some function specific to the plasma membrane. Since cellular plasma membranes face the cell's external environment, the membrane barriers must be very high to block

nonspecific permeation of small molecules across the membrane in both the inward and outward directions. Incorporation of cholesterol into the membrane serves this purpose well because cholesterol simultaneously raises hydrophobic barriers for polar molecules and increases rigidity barriers for nonpolar molecules. A change in hydrophobicity from the levels of propanol and octanol to those of hexane and hexadecane should greatly increase the activation energy required for polar and ionic small molecules to pass the membrane.

Effect of Cholesterol on Three-Dimensional Membrane Organization. The cholesterol molecule contains three well-distinguished regions: a small polar hydroxyl group, a rigid platelike steroid ring, and an alkyl chain tail. When cholesterol intercalates into the membrane, its polar hydroxyl group is positioned near the middle of the glycerol backbone region of the PC molecule (Worcetor & Franks, 1976). As shown in Figures 3, 4, and 5, the effect of cholesterol on hydrophobicity is remarkably depth-dependent, with a "turning point" at the eighth carbon for saturated-PC membranes (except DLPC, which has a turning point at the ninth carbon). Hydrophobicity decreases from the surface down to the seventh carbon and increases in the membrane deeper than the ninth carbon. This correlates well with the depth of penetration of the steroid ring structure of cholesterol, suggesting induction of packing defects near the surface region due to the cholesterol ring structure and dissolution of such defects in the central part of the membrane by the alkyl chains of PC and cholesterol.

In DOPC membranes, this transition point shifts to the 10th carbon, suggesting that the double bond between C9 and C10 of the oleoyl chains is involved in this shift. The steroid ring may penetrate to the 10th carbon, or the packing defects may persist up to the rigid 30° bend of oleoyl chains.

The width of the hydrophobic trapezoid in the presence of 50 mol % cholesterol is always narrower than that with 30 mol % cholesterol. This result may be explained by a high frequency of tail-to-tail apposition of cholesterol from both sides of the bilayer since the bulky steroid ring structure is short and the cross-section of the ring structure is much larger than that of the alkyl chain tail of cholesterol. McIntosh (1978) used X-ray diffraction to show that incorporation of 33 mol % cholesterol reduces the width of DSPC membranes while it increases the width of DPPC membranes in the gel phase. Sinking of cholesterol into the membrane may be accompanied by that of DSPC molecules because the higher exposure of the hydrocarbon chains may be energetically unfavorable.

Possibility of Hydrophobic Channeling and Enhanced Chemical Reactions in the Membrane. We previously studied transport (the product of local concentration and the local diffusion coefficient) of molecular oxygen and a hydrophobic square-planar copper complex (MW = 393.5, 8- × 8-Å square plate) in PC–cholesterol membranes (Subczynski et al., 1987). The hydrophobicity profiles obtained in the present study have many similarities with the profiles of the transport parameters for these hydrophobic small molecules (Subczynski et al., 1989, 1990, 1991). Increases in the transport parameters for these molecules parallel those in hydrophobicity, i.e., a decrease in water penetration. Therefore, the profile for the transport of small hydrophobic molecules is almost completely opposite that for water penetration. The only similarity between these two may be the effect of alkyl chain unsaturation, which reduces the transport of molecular oxygen and $CuKTSM_2$ as well as the extent of water penetration at all locations in the membrane.

These similarities between the transport profiles of small hydrophobic molecules and the hydrophobic profiles in the membrane suggest the possibility of lateral transport of nonpolar molecules along the inner core region of the membrane (parallel to the membrane), which is referred to as "hydrophobic channeling". For example, Skulachev (1990) noted the possibility of lateral transport of small hydrophobic solutes along the filamentous extended network of mitochondria.

The present results showed that water penetration into the membrane is extensive up to the depth of C8, even in the presence of cholesterol. Furthermore, even metal ions such as $Fe(CN)_6^{3-}$ can penetrate into the membrane to about the same depth. These results suggest that reactions involving both polar and nonpolar molecules can easily take place within the membrane. Biological membranes can thus provide a setting which facilitates various chemical reactions that cannot occur in the bulk phase.

The variations in hydrophobicity in the membrane may affect chemical reactions that are dependent on solvent polarity (Korytowski et al., 1992). For example, the reaction of singlet oxygen with cholesterol gives two different products, 3β-hydroxy-5α-cholest-6-ene-5-hydroperoxide and 3β-hydroxy-cholest-4-ene-6β-hydroperoxide, the yields of which depend on solvent polarity (Schenck et al., 1958). Local hydrophobicity (polarity) within the lipid bilayer should be taken into account in any investigation of chemical reactions associated with the membrane.

CONCLUSIONS

(1) The hydrophobicity profiles (levels of water penetration) correlate well with the permeability data for small polar molecules obtained previously by many researchers. These results indicate that the peak hydrophobicity in the center of the membrane is a hydrophobic barrier to permeation of small polar molecules, including water. In contrast, the rigidity barrier in the polar headgroup region and the near-surface region of the lipid membrane is more significant for permeation of nonpolar molecules.

(2) Saturated-PC membranes provide poor hydrophobic barriers. The polarities in the near-surface region and in the core region of the membrane are comparable to those for methanol (–ethanol) and 2-propanol, respectively, indicating low hydrophobicity (high polarity) with a dielectric constant between 10 and 30 in saturated-PC membranes.

(3) Introduction of either a *cis* or a *trans* double bond to the alkyl chain increases hydrophobicity at all locations in the membrane. The effect of the *cis* bond is greater. The effect is particularly marked in the center of the membrane, where polarity decreases to the level of dipropylamine, with a dielectric constant close to 3.

(4) Incorporation of cholesterol *increases* the extent of water penetration into both the polar headgroup region and the near-surface region in the hydrocarbon phase.

(5) Incorporation of 30 mol % cholesterol increases hydrophobicity from the ninth carbon inward in saturated-PC and DEPC membranes and from the 10th carbon inward in DOPC and EYPC membranes to the level of hexane and hexadecane. This taken together with conclusions 2 and 3 suggests that the lipid part of the membrane can be a significant hydrophobic barrier to permeation of polar molecules only when it includes unsaturated alkyl chains and/or cholesterol.

(6) Since cholesterol decreases hydrophobicity in the outer regions of the membrane (outside the seventh and ninth positions for saturated-PC (plus DEPC) and DOPC mem-

branes, respectively) and the transition from low to high hydrophobicity occurs very sharply within two carbons in the alkyl chain, the profiles appear almost rectangular.

(7) The above results were confirmed by studying the accessibility of $Fe(CN)_6^{3-}$ ion dissolved in water into DOPC–cholesterol membranes at 25 °C.

REFERENCES

Andrews, D. M., Haydon, D. A., & Fettiplace, R. (1971) *J. Membr. Biol. 5*, 277–296.

Bassolino-Klimas, D., Alper, H. E., & Stouch, T. R. (1993) *Biochemistry 32*, 12624–12637.

Blechner, S. L., Skita, V., & Rhodes, D. G. (1990) *Biochim. Biophys. Acta 1022*, 291–295.

Carruthers, A., & Melchior, D. L. (1983) *Biochemistry 22*, 5797–5807.

Chakrabarti, A. C., & Daemer, D. W. (1992) *Biochim. Biophys. Acta 1111*, 171–177.

Chaplin, D. B., & Kleinfeld, A. M. (1983) *Biochim. Biophys. Acta 731*, 465–474.

Cohen, A. H., & Hoffman, B. M. (1973) *J. Am. Chem. Soc. 95*, 2061–2062.

Daemer, D. W., & Bramhall, J. (1986) *Chem. Phys. Lipids 40*, 167–188.

Diamond, J. M., & Katz, Y. (1974) *J. Membr. Biol. 17*, 121–154.

Egret-Charlier, M., Sanson, A., Ptak, M., & Bouloussa, O. (1978) *FEBS Lett. 89*, 313–316.

Ellena, J. F., Archer, S. J., Dominey, R. N., Hill, B. D., & Cafiso, D. S. (1988) *Biochim. Biophys. Acta 940*, 63–70.

Fettiplace, R., Andrews, D. M., & Haydon, D. A. (1971) *J. Membr. Biol. 3*, 277–296.

Finkelstein, A. (1976) *J. Gen. Physiol. 68*, 127–135.

Franks, N. P., & Lieb, W. B. (1979) *J. Mol. Biol. 133*, 469–500.

Franks, N. P., & Lieb, W. B. (1980) *J. Mol. Biol. 141*, 43–61.

Fretten, P., Morris, S. J., Watts, A., & Marsh, D. (1980) *Biochim. Biophys. Acta 598*, 247–259.

Griffith, O. H., & Jost, P. C. (1976) in *Spin Labeling. Theory and Applications* (Berliner, L. J., Ed.) pp 453–523, Academic Press, New York.

Griffith, O. H., Dehlinger, P. J., & Van, S. P. (1974) *J. Membr. Biol. 15*, 159–192.

Hiff, T., & Kevan, L. (1989) *J. Phys. Chem. 93*, 1572–1575.

Higaki, K., Koto, M., Hashida, M., & Sezaki, H. (1988) *Pharm. Res. 5*, 309–312.

Ho, C., & Stubbs, C. D. (1992) *Biophys. J. 63*, 897–902.

Hyde, J. S., & Subczynski, W. K. (1989) *Biol. Magn. Reson. 8*, 399–425.

Johnson, M. E. (1981) *Biochemistry 20*, 3319–3328.

Koenig, S. H., Ahkong, Q. F., Brown, R. D., III, Lafleur, M., Spillar, M., Unger, E., & Tilcock, C. (1992) *Magn. Reson. Med. 23*, 275–286.

Korytowski, W., Bachowski, G. J., & Girotti, A. W. (1992) *Photochem. Photobiol. 56*, 1–8.

Kusumi, A., & Pasenkiewicz-Gierula, M. (1988) *Biochemistry 27*, 4407–4415.

Kusumi, A., Subczynski, W. K., & Hyde, J. S. (1982a) *Fed. Proc. 41*, 1394.

Kusumi, A., Subczynski, W. K., & Hyde, J. S. (1982b) *Proc. Natl. Acad. Sci. U.S.A. 79*, 1854–1858.

Kusumi, A., Tsuda, M., Akino, T., Ohnishi, S., & Terayama, Y. (1983) *Biochemistry 22*, 1165–1170.

Kusumi, A., Subczynski, W. K., Pasenkiewicz-Gierula, M., Hyde, J. S., & Merkle, H. (1986) *Biochim. Biophys. Acta 854*, 307–317.

Lassmann, G., Ebert, B., Kuznetsov, A. N., & Damerau, W. (1973) *Biochim. Biophys. Acta 310*, 298–304.

Lazrak, T., Milon, A., Wolff, G., Albrecht, A. M., Miehé, M., Ourisson, G., & Nakatani, Y. (1987) *Biochim. Biophys. Acta 1903*, 132–141.

Leahy, D. E., & Wait, A. R. (1986) *J. Pharm. Sci. 75*, 1157–1161.

Lieb, W. R., & Stein, W. D. (1986) *J. Membr. Biol. 92*, 111–119.

McIntosh, T. J. (1978) *Biochim. Biophys. Acta 513*, 43–58.

Merkle, H., Subczynski, W. K., & Kusumi, A. (1987) *Biochim. Biophys. Acta 897*, 238–248.

Milon, A., Lazrak, T., Albrecht, A. M., Wolff, G., Weill, G., Ourisson, G., & Nakatani, Y. (1986) *Biochim. Biophys. Acta 859*, 1–9.

Molin, Y. N., Salikhov, K. M., & Zamaraev, K. I. (1980) in *Spin Exchange*, Springer, Berlin.

Ohki, S. (1968) *J. Theor. Biol. 19*, 97–115.

Ohki, S. (1969) *Biophys. J. 9*, 1197–1205.

Overton, E. (1899) *Vierteljahrsschr. Naturforsch. Ges. Zürich 44*, 88–135.

Pasenkiewicz-Gierula, M., Hyde, J. S., & Pilbrow, J. R. (1983) *J. Magn. Reson. 55*, 255–265.

Pasenkiewicz-Gierula, M., Subczynski, W. K., & Kusumi, A. (1990) *Biochemistry 29*, 4059–5069.

Pasenkiewicz-Gierula, M., Subczynski, W. K., & Kusumi, A. (1991) *Biochimie 73*, 1311–1316.

Sanson, A., Ptak, M., Rignaud, J. L., & Gary-Boho, C. M. (1976) *Chem. Phys. Lipids 17*, 435–444.

Schenck, G. O., Neumullen, O. A., & Eisfeld, W. (1958) *Liebigs Ann. Chem. 618*, 202–210.

Seelig, J., & Waespa-Sarcevic, N. (1978) *Biochemistry 17*, 3310–3315.

Simon, S. A., McIntosh, T. J., & Latorre, R. (1982) *Science 216*, 65–67.

Skulachev, V. P. (1990) *J. Membr. Biol. 114*, 97–112.

Subczynski, W. K., Antholine, W. E., Hyde, J. S., & Petering, D. H. (1987) *J. Am. Chem. Soc. 109*, 46–52.

Subczynski, W. K., Hyde, J. S., & Kusumi, A. (1989) *Proc. Natl. Acad. Sci. U.S.A. 86*, 4474–4478.

Subczynski, W. K., Antholine, W. E., Hyde, J. S., & Kusumi, A. (1990) *Biochemistry 29*, 7936–7945.

Subczynski, W. K., Hyde, J. S., & Kusumi, A. (1991) *Biochemistry 30*, 8578–8590.

Subczynski, W. K., Hopwood, L. E., & Hyde, J. S. (1992) *J. Gen. Physiol. 100*, 1–19.

Träuble, H., & Eible, H. (1974) *Proc. Natl. Acad. Sci. U.S.A. 71*, 214–219.

Walter, A., & Gutknecht, J. (1986) *J. Membr. Biol. 90*, 207–217.

White, S. H. (1977) *Ann. N. Y. Acad. Sci. 303*, 243–265.

Windle, J. J. (1981) *J. Magn. Reson. 45*, 432–439.

Worcetor, D. L., & Franks, N. P. (1976) *J. Mol. Biol. 100*, 359–378.

Yin, J.-J., Pasenkiewicz-Gierula, M., & Hyde, J. S. (1987) *Proc. Natl. Acad. Sci. U.S.A. 84*, 964–968.

Zaccai, G., Blasie, J. K., & Schoenborn, B. P. (1975) *Proc. Natl. Acad. Sci. U.S.A. 72*, 376–380.